

Cite this: *Analyst*, 2015, **140**, 3766

# A near-infrared fluorescent probe for the detection of hydrogen polysulfides biosynthetic pathways in living cells and *in vivo*†

Min Gao,<sup>‡a,b</sup> Rui Wang,<sup>‡b</sup> Fabiao Yu,<sup>\*b</sup> Jinmao You<sup>a</sup> and Lingxin Chen<sup>\*a,b</sup>

Hydrogen polysulfides ( $\text{H}_2\text{S}_n$ ,  $n > 1$ ), derived from hydrogen sulfide ( $\text{H}_2\text{S}$ ), have been considered to be involved in cytoprotective processes and redox signaling. The emerging evidences imply that the actual signaling molecule is  $\text{H}_2\text{S}_n$  rather than  $\text{H}_2\text{S}$ . In this work, we present a near-infrared fluorescent probe BD-ss for the selective detection of  $\text{H}_2\text{S}_n$  biosynthetic pathways in living cells and *in vivo*. The probe is constructed by equipping a bis-electrophilic  $\text{H}_2\text{S}_n$  capture group *p*-nitrofluorobenzoate to a near-infrared fluorophore azo-BODIPY. BD-ss can provide a remarkable turn-on fluorescence response for assessing endogenous  $\text{H}_2\text{S}_n$  formation ways in serum, in living cells and *in vivo*.

Received 23rd December 2014,  
Accepted 17th March 2015

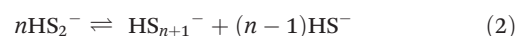
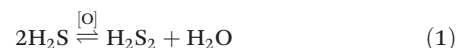
DOI: 10.1039/c4an02366h

www.rsc.org/analyst

## Introduction

The performance of reactive sulfur species (RSS) has involved in every aspect of cell biology, from protein function to redox signal transduction. More and more evidence indicates that a variety of diseases arise due to RSS dysregulation, which are modified with reactive oxygen and reactive nitrogen species (ROS and RNS).<sup>1</sup> RSS mainly include glutathione (GSH), cysteine (Cys), hydrogen sulphides ( $\text{H}_2\text{S}$ ), hydrogen polysulfides ( $\text{H}_2\text{S}_n$ ,  $n > 1$ ), persulfides, and *S*-modified cysteine adducts such as *S*-nitrosothiols and sulfenic acids. Among them,  $\text{H}_2\text{S}$  is now recognized as the third gasotransmitter that plays important roles in biological systems.<sup>2</sup> However,  $\text{H}_2\text{S}_n$ , the direct redox forms of  $\text{H}_2\text{S}$  which are considered to be involved in cytoprotective processes and redox signaling, have always drawn less attention, due to the lack of selective chemical tools. From the redox chemistry perspective, the redox couple of  $\text{H}_2\text{S}$  and  $\text{H}_2\text{S}_n$  is very likely to coexist in biological systems. In the presence of ROS,  $\text{H}_2\text{S}$  can form disulphide species. The disulphide species can also be reduced to  $\text{H}_2\text{S}$  (1). However, a disulphide species will rapidly undergo further redox equilibrium reactions to produce other hydrogen poly-

sulfides, which is controlled by pH and the relative amount of the oxidized *versus* reduced forms (2).<sup>3</sup>



At high (millimolar) concentrations, hydropolysulfides can also be formed by the autoxidation of  $\text{H}_2\text{S}$ .<sup>4</sup> It is worth noting that the biosynthetic pathways and biofunctions of  $\text{H}_2\text{S}_n$  are still under investigation.  $\text{H}_2\text{S}_n$  may have their own biosynthetic pathways from  $\text{H}_2\text{S}$  in the presence of ROS.<sup>3</sup>  $\text{H}_2\text{S}_n$  can also behave as the precursors of  $\text{H}_2\text{S}$  through their reducibility.<sup>5</sup> Therefore, some biological mechanisms that have previously been attributed to  $\text{H}_2\text{S}$  may actually be mediated by  $\text{H}_2\text{S}_n$ .<sup>4</sup> For example, polysulfides can activate transient receptor potential channels in astrocytes, which previously has been contributed to the activating of  $\text{H}_2\text{S}$ .

In order to better understand the function and biological properties of  $\text{H}_2\text{S}_n$ , it is urgent to develop highly selective and accurate methods for the detection of  $\text{H}_2\text{S}_n$  in biosystems. The traditional method for detecting polysulfides is to measure UV absorption peaks at 290–300 nm and 370 nm.<sup>6</sup> However, this traditional detection method requires the reduction of polysulfides to  $\text{H}_2\text{S}$ . Therefore, the traditional method cannot meet the demands of biological *in situ* detection by sensitivity and selectivity. Additionally,  $\text{H}_2\text{S}_n$  is the species in biosystems. For this reason, a fluorescent probe will be the desired chemical tool for the detection of intracellular  $\text{H}_2\text{S}_n$  because of its high sensitivity, selectivity and real-time detection.<sup>7</sup> Unfortunately, there are very few reports on fluorescent probes for  $\text{H}_2\text{S}_n$  detection, so far.<sup>8</sup> Xian's group has developed fluorescent probes with an emission located in the visible region for the selective

<sup>a</sup>The Key Laboratory of Life-Organic Analysis, College of Chemistry and Chemical Engineering, Qufu Normal University, Qufu 273165, China

<sup>b</sup>Key Laboratory of Coastal Environmental Processes and Ecological Remediation, The Research Centre for Coastal Environmental Engineering and Technology, Yantai Institute of Coastal Zone Research, Chinese Academy of Sciences, Yantai 264003, China. E-mail: fbyu@yic.ac.cn, lxchen@yic.ac.cn

†Electronic supplementary information (ESI) available: More experimental details. See DOI: 10.1039/c4an02366h

‡These authors contributed equally.



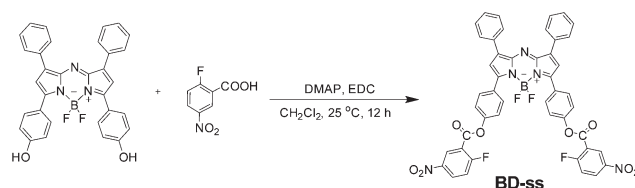
detection of exogenous  $\text{H}_2\text{S}_n$  in living cells. Compared with a short wavelength emission, near-infrared (NIR) light has drawn immense attention, because the NIR light can improve the tissue depth penetration and minimize the effect from the background autofluorescence.<sup>7,9</sup> With this in mind, we present a new NIR fluorescent probe for the detection of  $\text{H}_2\text{S}_n$  in living cells and *in vivo*.

## Results and discussion

### Probe design and detection mechanism

We conceive that  $\text{H}_2\text{S}_n$  hold two electrophilic mercapto groups ( $-\text{SH}$ ), that is, such compounds can perform bis-nucleophilic reactions in biological systems. This chemical property may provide an opportunity for the selective capture of  $\text{H}_2\text{S}_n$ . We selected a bis-electrophilic nitro-activated fluorobenzoate<sup>8a</sup> as the modulator for the probe BD-ss (Scheme 2). Electrophilic groups are often considered to be a strong quencher for the fluorophore. Therefore, we anticipate that the fluorescence properties of a fluorophore can be manipulated through a photoinduced electron transfer (PET) process from the excited fluorophore to the strong electron-withdrawing group (donor-excited PET, d-PET).<sup>10</sup> To achieve our design strategy, we particularly chose azo-BODIPY as the fluorophore, because of its high molar absorption coefficient, good photostability, and NIR emission. After the integration of the nitro-activated fluorobenzoate into the azo-BODIPY platform, the fluorescence of the fluorophore is effectively quenched by the d-PET process between the modulator and the fluorophore.

$\text{H}_2\text{S}_n$  include a large number of active species, however, there exists a rapid dynamic equilibrium between them (Scheme 1).<sup>11</sup> Therefore, in this work, hydrogen disulfide ( $\text{H}_2\text{S}_2$ ) is always used as the primary model compound of  $\text{H}_2\text{S}_n$ . In our experiments, freshly prepared solutions of  $\text{Na}_2\text{S}_2$  were used as the source of  $\text{H}_2\text{S}_2$ . The proposed detection mechanism of BD-ss is illustrated in Scheme 1.  $\text{H}_2\text{S}_2$  begins a nucleophilic aromatic substitution ( $\text{S}_\text{N}\text{Ar}$ ) *via* replacing a F-atom to form an intermediate containing a free  $-\text{SH}$  group. Subsequently, the free  $-\text{SH}$  group undergoes a spontaneous intramolecular cyclization with the ester group to release the azo-BODIPY fluorophore. This tandem reaction will eliminate the d-PET process, and trigger the fluorescence switch turn-on significantly. In order to affirm the detection mechanism of our probe, we performed the reaction of BD-ss with a biothiol



Scheme 2 Synthetic route of BD-ss.

model *N*-acetyl-L-cysteine methyl ester. The fluorescent intensity did not change when the *N*-acetyl-L-cysteine methyl ester was added. However, after  $\text{Na}_2\text{S}_2$  was added to the reaction mixture, as expected, a remarkable increase in the fluorescence intensity was observed. The results indicate that the relevant biothiols cannot interfere with the detection of  $\text{H}_2\text{S}_n$  (Scheme S1, ESI†).

### Spectroscopic properties

The absorption and fluorescence spectra of BD-ss (10  $\mu\text{M}$ ) were examined under simulated physiological conditions (10 mM HEPES buffer, pH 7.4). As is well recognized, the environment of the cell is liposoluble, so we employed 0.4% Tween 80 to simulate the hydrophobicity of the cells, since Tween 80 is a nonionic surfactant and has been widely used in foods, pharmaceutical preparations, and cosmetics due to its effectiveness at low concentrations and relatively low toxicity. BD-ss exhibited an absorption peak centred at 660 nm ( $\epsilon_{660 \text{ nm}} = 3.2 \times 10^5 \text{ cm}^{-1} \text{ M}^{-1}$ ). After treatment BD-ss with  $\text{Na}_2\text{S}_2$ , a new absorption peak appeared at 707 nm ( $\epsilon_{707 \text{ nm}} = 3.6 \times 10^5 \text{ cm}^{-1} \text{ M}^{-1}$ ) indicating that BD-ss had reacted with  $\text{H}_2\text{S}_2$  and induced the cleavage of the ester group to release the fluorophore (Fig. 1). Upon the addition of different concentration of  $\text{Na}_2\text{S}_2$  (0–20  $\mu\text{M}$ ), the fluorescent profile gradually increased in the NIR region (Fig. 2a). The fluorescence intensities at 737 nm were linearly related to the concentrations of  $\text{Na}_2\text{S}_2$  under the given range (Fig. 2b). The regression equation was  $F_{737 \text{ nm}} = 3.56 \times 10^5 [\text{Na}_2\text{S}_2] \mu\text{M} + 1.48 \times 10^5$  with  $r = 0.9970$ . The detection limit was determined to be 50 nM ( $3\sigma/\kappa$ ) under the experimental conditions. The results demonstrate that BD-ss can potentially detect  $\text{H}_2\text{S}_n$  both qualitatively and quantitatively

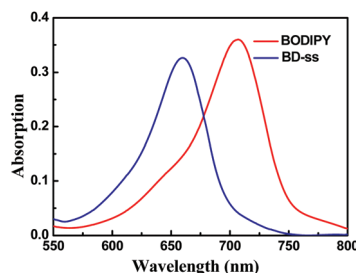
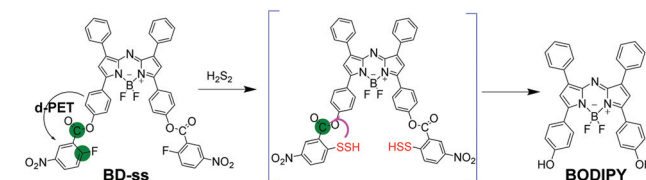
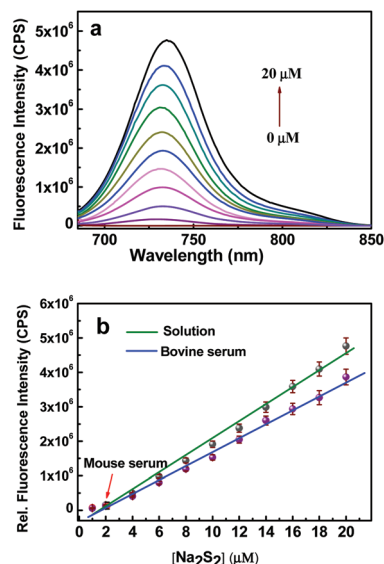


Fig. 1 UV-vis absorption spectral of probe BD-ss (10  $\mu\text{M}$ ) before and after addition of  $\text{Na}_2\text{S}_2$  (20  $\mu\text{M}$ ). The blue curve is the absorption spectrum of BD-ss. The red curve was recorded after treatment with  $\text{Na}_2\text{S}_2$ .



Scheme 1 Structure of BD-ss and proposed mechanism of BD-ss against  $\text{H}_2\text{S}_2$ .





**Fig. 2** (a) Fluorescence spectra of BD-ss (10  $\mu\text{M}$ ) upon addition of  $\text{Na}_2\text{S}_2$  (0–20  $\mu\text{M}$ ). Spectra were acquired in 10 mM HEPES buffer (pH 7.4, 0.4% Tween 80) after incubation with various concentrations of  $\text{Na}_2\text{S}_2$  for 5 min at 37  $^\circ\text{C}$ . (b) The corresponding linear relationship between the fluorescent intensity and  $\text{Na}_2\text{S}_2$  concentrations (0–20  $\mu\text{M}$ ) in buffer solution and in serum.  $\lambda_{\text{ex}} = 707 \text{ nm}$ ,  $\lambda_{\text{em}} = 737 \text{ nm}$ . The red point is the mean fluorescence intensity in mice serum.

under simulated physiological conditions. We also explored the ability of BD-ss to quantify  $\text{H}_2\text{S}_n$  in a serum sample. We prepared a simulated solution containing 20% fetal bovine serum to test the probe. Different concentrations of  $\text{Na}_2\text{S}_2$  (0–20  $\mu\text{M}$ ) were added to the samples containing BD-ss (10  $\mu\text{M}$ ). As shown in Fig. 2b, the fluorescence intensities at 737 nm were linearly related to the concentration of  $\text{Na}_2\text{S}_2$ . The regression equation was  $F_{737 \text{ nm}} = 2.08 \times 10^5 [\text{Na}_2\text{S}_2] \mu\text{M} - 3.30 \times 10^3$ , with  $r = 0.9945$ . The different profiles of the two calibration curves could be attributed to the reaction between  $\text{H}_2\text{S}_n$  and the biomolecules in the serum. The result indicates that our probe can determine  $\text{H}_2\text{S}_n$  both qualitatively and quantitatively in serum.

The physiologically relevant  $\text{H}_2\text{S}$  concentration is estimated ranging from the nano- to millimolar levels.<sup>2</sup> However, the endogenous  $\text{H}_2\text{S}$  metabolism can be reversed through an oxygen-dependent sulfane sulfur production. Sulfane sulfur is an uncharged form of sulfur ( $\text{S}^0$ ) with six valence electrons, which can be reversibly attached to proteins *via* a covalent bond between the  $\text{S}^0$  and other sulfur atoms. They are mainly present in dihydropolysulfides ( $\text{H-S}_n\text{-SH}$ ,  $n \geq 1$ ), hydropolysulfides ( $\text{R-S}_n\text{-SH}$ ,  $n \geq 1$ ), polysulfides ( $\text{R-S-S}_n\text{-S-R}$ ,  $n \geq 1$ ), and elemental sulfur ( $\text{S}_8$ ).<sup>2c</sup> Sulfane sulfur plays important roles *in vivo*. To completely comprehend the biofunctions of sulfane sulfur *in vivo*, it is necessary to develop methods that are sensitive enough to evaluate sulfane sulfur levels in biological samples. The traditional methods for the total sulfane sulfur assessment offer the concentrations ranging 1.3 to 85  $\mu\text{M}$ .<sup>12</sup> As far as we know, to date, the concentration of  $\text{H}_2\text{S}_n$  is unavailable.

Therefore, we next applied our probe to directly detect  $\text{H}_2\text{S}_n$  concentration in the BALB/c mouse serum ( $n = 5$ ). The concentration of  $\text{H}_2\text{S}_n$  in the serum of mice was 2.01  $\mu\text{M}$  (the red point in Fig. 2b). Our calibration curve covers the range of endogenous levels of  $\text{H}_2\text{S}_n$ , which indicates that our probe is suitable for the detection of  $\text{H}_2\text{S}_n$  in biological samples.

### Selectivity to $\text{H}_2\text{S}_n$

To test the selectivity for  $\text{H}_2\text{S}_n$ , BD-ss was treated with a series of biorelated RSS. As shown in Fig. 3, only  $\text{H}_2\text{S}_n$  could trigger strong fluorescence response. Other RSS, such as Cys, Hcy, GSH, CysSSCys, GSSG, Cys-poly-sulfide,  $\text{S}_8$ ,  $\text{S}_2\text{O}_3^{2-}$  and  $\text{HSO}_3^-$ , could not induce any fluorescence increase. However, NaHS (a common source of  $\text{H}_2\text{S}$ ) caused a small enhancement in the fluorescence intensity, due to the autoxidation of  $\text{H}_2\text{S}$  to  $\text{H}_2\text{S}_n$  at high concentrations.<sup>5</sup> We also tested the response of BD-ss to other reductive species, such as ascorbic acid and tocopherol. There was also no fluorescence response to be found. Additionally, we also tested whether the effect of common physiological metal ions and anions could induce interference, or not. As shown in Fig. S5 (see ESI<sup>†</sup>), the probe did not give any fluorescence response to these metal ions and anions. Since the probe showed a high selectivity towards  $\text{H}_2\text{S}_n$ , the competition experiments were performed in the presence of  $\text{Na}_2\text{S}_2$ . When  $\text{Na}_2\text{S}_2$  (10  $\mu\text{M}$ ) and other RSS coexisted, we still observed a satisfactory fluorescence response. These results demonstrate that our probe can be used for the selective detection of  $\text{H}_2\text{S}_n$  in the presence of biothiols and other physiological species.

### Biosynthetic pathways of $\text{H}_2\text{S}_n$

The biosynthetic pathways of  $\text{H}_2\text{S}_n$  are under investigation; recent studies suggest that  $\text{H}_2\text{S}_n$  may be derived from  $\text{H}_2\text{S}$  in the presence of ROS.<sup>3,13</sup> We next employed BD-ss to detect

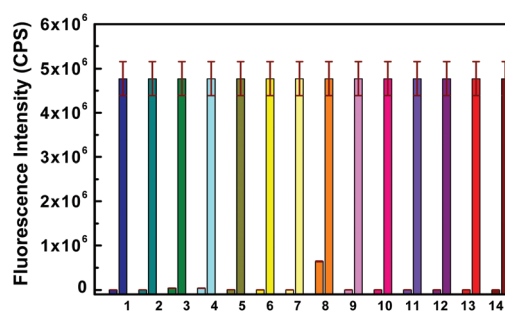


**Fig. 3** Fluorescence responses of BD-ss (10  $\mu\text{M}$ ) to biologically relevant RSS. In each group, the bars represent relative responses at 737 nm of BD-ss to RSS and the mixture of RSS with 10  $\mu\text{M}$   $\text{Na}_2\text{S}_2$ , respectively. Legend: (1) blank + 20  $\mu\text{M}$   $\text{Na}_2\text{S}_2$ ; (2) blank + 20  $\mu\text{M}$   $\text{Na}_2\text{S}_4$ ; (3) 1 mM Cys +  $\text{Na}_2\text{S}_2$ ; (4) 1 mM Hcy +  $\text{Na}_2\text{S}_2$ ; (5) 10 mM GSH +  $\text{Na}_2\text{S}_2$ ; (6) 1 mM CysSSCys +  $\text{Na}_2\text{S}_2$ ; (7) 1 mM GSSG +  $\text{Na}_2\text{S}_2$ ; (8) 0.5 mM NaHS +  $\text{Na}_2\text{S}_2$ ; (9) 1 mM Cys-poly-sulfide +  $\text{Na}_2\text{S}_2$ ; (10) 0.5 mM  $\text{S}_8$  +  $\text{Na}_2\text{S}_2$ ; (11) 0.5 mM  $\text{Na}_2\text{S}_2\text{O}_3$  +  $\text{Na}_2\text{S}_2$ ; (12) 0.5 mM  $\text{NaHSO}_3$  +  $\text{Na}_2\text{S}_2$ ; (13) 1 mM ascorbic acid +  $\text{Na}_2\text{S}_2$ ; (14) 1 mM tocopherol +  $\text{Na}_2\text{S}_2$ . Data were recorded in 10 mM HEPES buffer (pH 7.4 and 0.4% Tween 80) at 37  $^\circ\text{C}$  for 35 min.  $\lambda_{\text{ex}} = 707 \text{ nm}$ ,  $\lambda_{\text{em}} = 737 \text{ nm}$ .



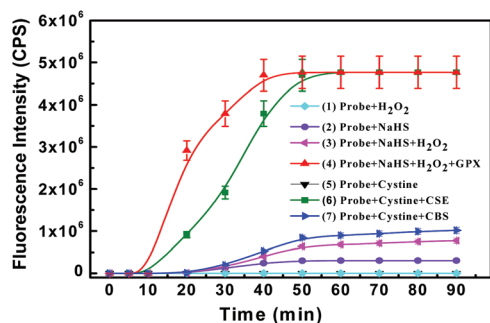


**Fig. 4** Fluorescence responses of BD-ss (10  $\mu\text{M}$ ) towards (1)–(4)  $\text{H}_2\text{O}_2$  (50  $\mu\text{M}$ ) in the presence of NaHS (50  $\mu\text{M}$ ) or GPx (50  $\text{U L}^{-1}$ ), and (5)–(7) hydrogen polysulfides catalysed by CSE (50  $\mu\text{g mL}^{-1}$ ) and CBS (5  $\mu\text{g mL}^{-1}$ ) using cystine (1.25 mM) as a substrate. Data were acquired in 10 mM HEPES buffer (pH 7.4, 0.4% Tween 80) at 37  $^\circ\text{C}$  for 35 min.  $\lambda_{\text{ex}}$  = 707 nm,  $\lambda_{\text{em}}$  = 737 nm.

*in situ*  $\text{H}_2\text{S}_n$  generation from  $\text{H}_2\text{S}$  and ROS. In this work,  $\text{H}_2\text{O}_2$  was chosen on behalf of ROS. As shown in Fig. 4, the probe BD-ss displayed no response to  $\text{H}_2\text{O}_2$ . When NaHS was premixed with  $\text{H}_2\text{O}_2$ , a small fluorescence enhancement was obtained, which indicated the formation of  $\text{H}_2\text{S}_n$  in the systems. However, the formation process for  $\text{H}_2\text{S}_n$  was very slow. It was reported that glutathione peroxidase (GPx) could scavenge ROS through converting reduced biothiols (RSH) to oxidized biothiols (RSSR),<sup>14</sup> which prompted us to consider that GPx might be involved in the  $\text{H}_2\text{S}_n$  biosynthesis. We added GPx to the system as a catalyst. Excitingly, a remarkable increase in the fluorescence intensity was observed within 20 min (Fig. 4), which demonstrated that GPx participated in the reaction between  $\text{H}_2\text{O}_2$  and  $\text{H}_2\text{S}$ . Moreover, some reports suggest that persulfides can be synthesized from cystine through cystathionine  $\gamma$ -lyase (CSE).<sup>15</sup> Therefore, we applied the probe to examine if  $\text{H}_2\text{S}_n$  could generate *via* enzymatic activity, including enzyme CSE and the related enzyme cystathionine  $\beta$ -synthase (CBS). As indicated in Fig. 4, both the enzymes CSE and CBS could induce a fluorescence intensity increase when cystine was used as a substrate, while the fluorescence response to CBS was much weaker than that of CSE. We attributed this phenomenon to the different physiological functions of the enzymes CSE and CBS in biosystems. The reaction of the enzyme CSE with cystine mainly focused on the derived hydropolysulfide species, while the enzyme CBS firstly generated polysulfides and then converted these to hydropolysulfides in the presence of cystine and glutathione.<sup>5,15</sup> All of these results illustrate that our probe is suitable for the detection of  $\text{H}_2\text{S}_n$  not only generated from ROS and  $\text{H}_2\text{S}$ , but also enzymatically produced in biochemical systems.

### Imaging $\text{H}_2\text{S}_n$ in cells

Having demonstrated the selectivity and sensitivity of BD-ss for  $\text{H}_2\text{S}_n$ , we next assessed the ability of BD-ss to respond to  $\text{H}_2\text{S}_n$  in the mouse macrophage cell line RAW264.7 cells. The first group (Fig. 5a–e): RAW264.7 cells were incubated with BD-

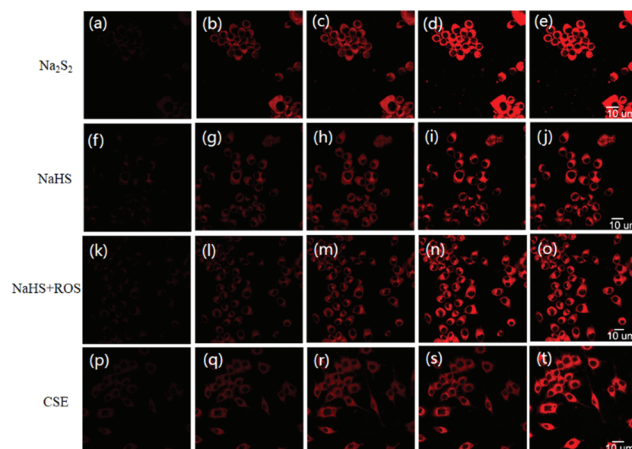


**Fig. 5** Confocal microscopy images of living RAW264.7 cells for visualizing  $\text{H}_2\text{S}_n$  level changes using BD-ss (1  $\mu\text{M}$ ). Images displayed represent emission intensity collected in optical window between 700 and 800 nm upon excitation at 635 nm. (a), (f), and (p) RAW264.7 cells incubated with BD-ss for 15 min at 37  $^\circ\text{C}$ , and washed with RPMI-1640. (b)–(e) The cells incubated with 5  $\mu\text{M}$   $\text{Na}_2\text{S}_2$  for 6 min, 9 min, 15 min, and 20 min at 37  $^\circ\text{C}$ . (g)–(j) RAW264.7 cells incubated with NaHS (50  $\mu\text{M}$ ) for 0.5 h, 1 h, 2 h, and 3 h at 37  $^\circ\text{C}$ . (k) The cells pretreated with PMA (10 nM) for 30 min to overproduce ROS. (l)–(o) the cells were incubated with NaHS (50  $\mu\text{M}$ ) for 3, 6, 8, and 15 min. (q)–(t) RAW264.7 cells were stimulated by LPS (1  $\mu\text{g mL}^{-1}$ ) to monitor  $\text{H}_2\text{S}_n$  produced endogenously for 8 h, 9 h, 10 h, and 16 h.

ss (1  $\mu\text{M}$ ) for 15 min at 37  $^\circ\text{C}$  as a control (Fig. 5a). The fluorescence intensity increased rapidly after the cells were incubated with  $\text{Na}_2\text{S}_2$  (5  $\mu\text{M}$ ) for 6 min, 9 min, 15 min, and 20 min at 37  $^\circ\text{C}$  (Fig. 5b–e). The fluorescence intensity was saturated after being incubated  $\text{Na}_2\text{S}_2$  for 15 min (Fig. 6a). The results illustrate that BD-ss can be used for detecting exogenously added  $\text{H}_2\text{S}_n$  in living cells. It has been reported that  $\text{H}_2\text{S}$  can be stored as  $\text{H}_2\text{S}_n$  in a sulfane sulfur pool when  $\text{H}_2\text{S}$  is at a high concentration.<sup>16</sup> Next, we applied our probe to monitor

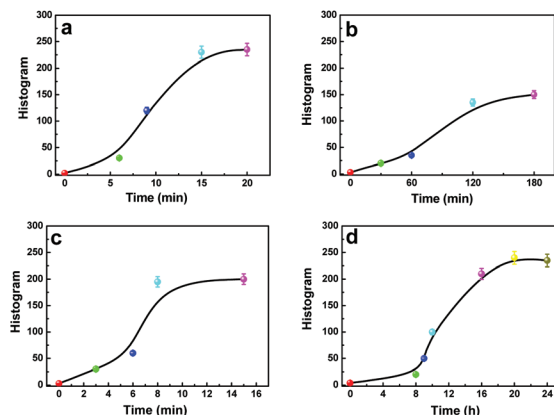


**Fig. 6** Histogram of time dependent intensities of the images in Fig. 5. (a) The histogram of Fig. 5a–e; (b) The histogram of Fig. 5f–j; (c) The histogram of Fig. 5k–o; (d) The histogram of Fig. 5p–t.



the conversion process of  $\text{H}_2\text{S}$  to  $\text{H}_2\text{S}_n$  over time in RAW264.7 cells. The cells in Fig. 5f were incubated with BD-ss for 15 min at 37 °C, and then washed with RPMI-1640. The cells were further incubated with NaHS (50  $\mu\text{M}$ ) for 0.5 h, 1 h, 2 h, and 3 h at 37 °C, respectively. As shown in Fig. 5g–j, the confocal fluorescence images grew brighter as the incubation time increased from 0.5 to 3 h (Fig. 6b). The results indicate that the cells can convert excess  $\text{H}_2\text{S}$  to  $\text{H}_2\text{S}_n$ .

Hitherto, the biosynthetic pathways of  $\text{H}_2\text{S}_n$  are far from indubitability. Some investigations propose that  $\text{H}_2\text{S}_n$  can be formed when  $\text{H}_2\text{S}$  reacts with ROS, such as  $\text{HClO}$ , and  $\text{H}_2\text{O}_2$ .<sup>3,11,13</sup> *In vitro* test, we also confirmed that  $\text{H}_2\text{S}_n$  could be derived from  $\text{H}_2\text{S}$  in the presence of  $\text{H}_2\text{O}_2$ , which is catalysed by GPx. Therefore, we turned our attention to verify  $\text{H}_2\text{S}_n$  production from ROS and  $\text{H}_2\text{S}$  in RAW264.7 cells. The cells in Fig. 5k were pretreated with phorbol 12-myristate 13-acetate (PMA, 10 nM) for 30 min to stimulate the overproduction of ROS.<sup>17</sup> Then, the cells incubated with BD-ss for 15 min. After being washed with RPMI-1640 to remove excess BD-ss, the cells were incubated with NaHS (50  $\mu\text{M}$ ) for 3, 6, 8, and 15 min (Fig. 5l–o). As expected, the fluorescence intensity increased (Fig. 6c), which provided a clear demonstration that ROS could react with  $\text{H}_2\text{S}$  to form  $\text{H}_2\text{S}_n$  using GPx as a catalyst in living cells due to RAW264.7 cells containing GPx to regulate antioxidant and anti-inflammatory activities.

After having confirmed the detection of  $\text{H}_2\text{S}_n$  supplemented exogenously, we next assessed the capability of BD-ss to detect endogenous  $\text{H}_2\text{S}_n$ . The formation of intracellular  $\text{H}_2\text{S}_n$  may be closely related with cystine and cystathionine  $\gamma$ -lyase (CSE).<sup>5,15</sup> We sought to determine whether our probe could detect endogenous  $\text{H}_2\text{S}_n$  that was derived from cystine and CSE in RAW264.7 cells. CSE mRNA can be overexpressed when induced by lipopolysaccharide (LPS) in RAW264.7 cells.<sup>18</sup> RAW264.7 cells were incubated with BD-ss for 15 min. After being washed with RPMI-1640, the cells were stimulated with LPS (1  $\mu\text{g mL}^{-1}$ ). We selected the time points of 8 h, 9 h, 10 h, and 16 h to monitor the production of endogenous  $\text{H}_2\text{S}_n$  (Fig. 5q–t). As expected, there existed an obvious fluorescence intensity increase over time (Fig. 6d). As a control experiment, the cells were pretreated with a CSE inhibitor, DL-propargylglycine (PAG, 1 mM),<sup>19</sup> and were incubated with BD-ss (1  $\mu\text{M}$ ) for 15 min. Subsequently, the cells were stimulated with LPS for 24 h. As shown in Fig. 7, the cells gave an attenuated fluorescence response, confirming that CSE contributed to the  $\text{H}_2\text{S}_n$  generation. All these results indicate that our probe can directly detect endogenous and exogenous  $\text{H}_2\text{S}_n$  level changes in living cells.

### Imaging $\text{H}_2\text{S}_n$ *in vivo*

In order to highlight the advantages of our NIR probe, we finally assessed the capability of BD-ss for visualizing  $\text{H}_2\text{S}_n$  formation in living animals. We utilized BALB/c mice as the biological model to examine the potentiality. The mice in Fig. 8a (group b) were injected in the intraperitoneal (i.p.) cavity with LPS (100  $\mu\text{L}$ , 10  $\mu\text{g mL}^{-1}$ ) for 24 h to induce CSE mRNA overexpression.<sup>18</sup> Then, these mice were loaded with BD-ss (50  $\mu\text{L}$ ,

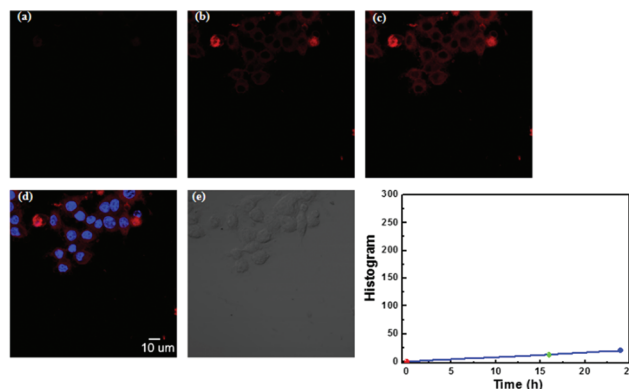


**Fig. 7** Fluorescence confocal microscopic images of RAW264.7 cells pretreated by the CSE inhibitor. The cells were treated DL-propargylglycine (1 mmol  $\text{L}^{-1}$ ) for 8 h, and then washed with RPMI-1640 and loaded with 1  $\mu\text{M}$  BD-ss under 37 °C for 15 min (a). The cells were next incubated with LPS (1  $\mu\text{g mL}^{-1}$ ). The cells showed much weaker fluorescence response at (b) 16 h and (c) 24 h.

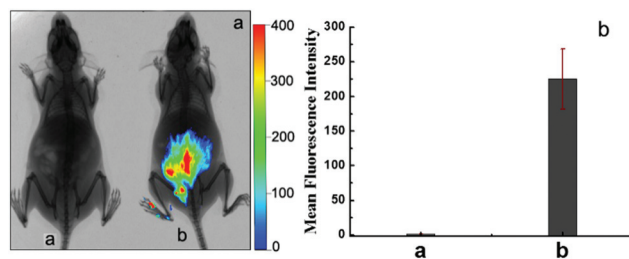


**Fig. 8** Representative fluorescence images of mice visualizing  $\text{H}_2\text{S}_n$  level changes using BD-ss. Images constructed from 720 nm fluorescence collection window,  $\lambda_{\text{ex}} = 710$  nm. (a) Group a was injected i.p. with BD-ss (10  $\mu\text{M}$ , 50  $\mu\text{L}$  in 1 : 9 DMSO–saline v/v) for 30 min. Group b was injected i.p. with LPS (10  $\mu\text{g mL}^{-1}$ , 100  $\mu\text{L}$  in 1 : 9 DMSO–saline v/v) for 24 h, and then loaded with BD-ss (10  $\mu\text{M}$ , 50  $\mu\text{L}$  in 1 : 9 DMSO–saline v/v) for 30 min. (b) Quantification of total photon flux from each group. The total number of photons from the entire peritoneal cavity of the mice was integrated.  $n = 5$ , Error bars are  $\pm\text{SEM}$ .

10  $\mu\text{M}$ ) for the next 30 min. There was a dramatic fluorescence increase in group b. The control mice which were given an i.p. injection of BD-ss (50  $\mu\text{L}$ , 10  $\mu\text{M}$ ) displayed a faint fluorescence (group a). The results indicated that our probe can detect the endogenous  $\text{H}_2\text{S}_n$  formation *in vivo*. Moreover, the quantification of the mean fluorescence intensities for each group are shown in Fig. 8b. The mean fluorescence intensity of group b is  $\sim 180$  times higher than that of the control group. All these results demonstrate that our probe can be used to image  $\text{H}_2\text{S}_n$  in living animals, which revealed the potential application of the new near-infrared fluorescent probe *in vivo*.

## Conclusions

In summary, we have developed a new NIR fluorescent probe BD-ss which exhibits a high selectivity and sensitivity for  $\text{H}_2\text{S}_n$  both in serum, in living cells and *in vivo*. The probe is con-



structed by equipping a bis-electrophilic  $\text{H}_2\text{S}_n$  capture group *p*-nitrofluorobenzoate to a near-infrared azo-BODIPY fluorophore. When exposed to  $\text{H}_2\text{S}_n$ , BD-ss releases a remarkable turn-on fluorescence response. In addition, BD-ss can also be used for monitoring  $\text{H}_2\text{S}_n$  in living cells not only exogenously added, but also produced *via* enzymatic stimulation. This successful example will open up a new avenue to develop promising probes for the advancement of bioimaging of  $\text{H}_2\text{S}_n$ .

## Experimental section

### Synthesis and characterization of probe BD-ss

BODIPY was synthesized in our laboratory according to the reported protocol.<sup>20</sup> A mixture of BODIPY (53.0 mg, 0.1 mmol), 2-fluoro-5-nitrobenzoic acid (37.0 mg, 0.2 mmol), 1-ethyl-3-(3-dimethylaminopropyl)carbodiimide hydrochloride (EDC, 38.4 mg, 0.2 mmol) and 4-dimethylaminopyridine (DMAP, 2.44 mg, 0.02 mmol) in  $\text{CH}_2\text{Cl}_2$  (50 mL) was stirred for 12 hours at 25 °C.<sup>20</sup> Then the mixture was neutralized with dilute HBr, and partitioned between  $\text{CH}_2\text{Cl}_2$  (50 mL) and  $\text{H}_2\text{O}$  (50 mL). Then, the organic phase was evaporated under reduced pressure and the resulting residue was subjected to column chromatography for purification ( $\text{CH}_2\text{Cl}_2$ ). The probe BD-ss was obtained as a green solid. Yield: 37.4 mg, 43.3%. <sup>1</sup>H NMR (500 MHz,  $\text{CDCl}_3\text{-D}_1$ )  $\delta$ (ppm): 8.11 (m, 2H), 8.02 (m, 2H), 7.65–7.36 (m, 15H), 7.24–7.20 (m, 5H), 7.19 (s, 1H), 4.25 (s, 1H). <sup>13</sup>C NMR (125 MHz,  $\text{CDCl}_3\text{-D}_1$ )  $\delta$ (ppm): 166.80, 165.01, 163.19, 157.22, 156.03, 153.97, 153.45, 152.05, 142.67, 136.15, 134.32, 132.15, 131.01, 130.59, 130.08, 129.45, 129.04, 128.95, 128.54, 128.20, 127.95, 127.15, 121.75, 121.03, 117.75, 117.36, 92.30. LC-MS (ESI<sup>+</sup>): *m/z*  $\text{C}_{46}\text{H}_{26}\text{BF}_4\text{N}_5\text{O}_8$  calcd 863.1811, found [*M*<sup>+</sup>] 863.1813.

## Acknowledgements

We thank the National Nature Science Foundation of China (NSFC) no. 21405172, no. 21275158, the Innovation Projects of the CAS (grant KZCX2-EW-206), and the program of Youth Innovation Promotion Association, CAS (grant 2015170).

## Notes and references

- (a) K. Miranda and D. Wink, *Proc. Natl. Acad. Sci. U. S. A.*, 2014, **111**, 7505; (b) G. Giles, K. Tasker and C. Jacob, *Free Radicals Biol. Med.*, 2001, **31**, 1279; (c) P. Nagy and M. T. Ashby, *J. Am. Chem. Soc.*, 2007, **129**, 14082.
- (a) V. Lin and C. Chang, *Curr. Opin. Chem. Biol.*, 2012, **16**, 595; (b) N. Francoleon, S. Carrington and J. Fukuto, *Arch. Biochem. Biophys.*, 2011, **516**, 146; (c) B. Paul and S. Snyder, *Nat. Rev. Mol. Cell Biol.*, 2012, **13**, 499; (d) R. Wang, *Physiol. Rev.*, 2012, **92**, 791; (e) P. Moore, M. Bhatia and S. Mochhala, *Trends Pharmacol. Sci.*, 2003, **24**, 609; (f) F. Yu, P. Li, P. Song, B. Wang, J. Zhao and K. Han, *Chem. Commun.*, 2012, **48**, 2852; (g) R. Wang, F. Yu, L. Chen, H. Chen, L. Wang and W. Zhang, *Chem. Commun.*, 2012, **48**, 11757; (h) F. Yu, X. Han and L. Chen, *Chem. Commun.*, 2014, **50**, 12234; (i) J. Liu, Y. Sun, J. Zhang, T. Yang, J. Cao, L. Zhang and W. Guo, *Chem. Commun.*, 2013, **19**, 4717; (j) W. Sun, J. Fan, C. Hu, J. Cao, H. Zhang, X. Xiong, J. Wang, S. Cui, S. Sun and X. Peng, *Chem. Commun.*, 2013, **49**, 3890.
- (a) P. Nagy and C. Winterbourn, *Chem. Res. Toxicol.*, 2010, **23**, 1541; (b) B. Predmore, D. Lefer and G. Gojon, *Antioxid. Redox Signaling*, 2012, **17**, 119; (c) T. Chatterji, K. Keerthi and K. Gates, *Bioorg. Med. Chem. Lett.*, 2005, **15**, 3921.
- (a) T. Ida, T. Sawa, H. Ihara, Y. Tsuchiya, Y. Watanabe, Y. Kumagai, M. Suematsu, H. Motohashi, S. Fujii, T. Matsunaga, M. Yamamoto, K. Ono, N. O. Devarie-Baez, M. Xian, J. M. Fukuto and T. Akaike, *Proc. Natl. Acad. Sci. U. S. A.*, 2014, **111**, 7606; (b) K. Ono, T. Akaike, T. Sawa, Y. Kumagai, D. A. Wink, D. J. Tantillo, A. J. Hobbs, P. Nagy, M. Xian, J. Lin and J. M. Fukuto, *Free Radicals Biol. Med.*, 2014, **77**, 82; (c) I. Artaud and E. Galardon, *ChemBioChem*, 2014, **15**, 2361; (d) T. S. Bailey, L. N. Zakharov and M. D. Pluth, *J. Am. Chem. Soc.*, 2014, **136**, 10573.
- (a) M. Jackson, S. Melideo and M. Jorns, *Biochemistry*, 2012, **51**, 6804; (b) M. Ishigami, K. Hiraki, K. Umemura, Y. Ogasawara, K. Ishii and H. Kimura, *Antioxid. Redox Signaling*, 2009, **11**, 205.
- R. Greiner, Z. Pálkás, K. Bäsell, D. Becher, H. Antelmann, P. Nagy and T. Dick, *Antioxid. Redox Signaling*, 2013, **19**, 1749.
- (a) C. Liu, J. Pan, S. Li, Y. Zhao, L. Wu, C. E. Berkman, A. R. Whorton and M. Xian, *Angew. Chem., Int. Ed.*, 2011, **50**, 10327; (b) X. Chen, Y. Zhou, X. Peng and J. Yoon, *Chem. Soc. Rev.*, 2010, **39**, 2120; (c) X. Li, X. Gao, W. Shi and H. Ma, *Chem. Rev.*, 2014, **114**, 590; (d) C. E. Paulsen and K. S. Carroll, *Chem. Rev.*, 2013, **113**, 4633; (e) Y. Yang, Q. Zhao, W. Feng and F. Li, *Chem. Rev.*, 2013, **113**, 192; (f) L. Yuan, W. Lin, K. Zheng, L. He and W. Huang, *Chem. Soc. Rev.*, 2012, **42**, 622; (g) J. Fan, M. Hu, P. Zhan and X. Peng, *Chem. Soc. Rev.*, 2013, **42**, 29; (h) J. Chan, S. C. Dodani and C. J. Chang, *Nat. Chem.*, 2012, **4**, 973.
- (a) C. Liu, W. Chen, W. Shi, B. Peng, Y. Zhao, H. Ma and M. Xian, *J. Am. Chem. Soc.*, 2014, **136**, 7257; (b) W. Chen, C. Liu, B. Peng, Y. Zhao, A. Pacheco and M. Xian, *Chem. Sci.*, 2013, **4**, 2892; (c) L. Zeng, S. Chen, T. Xia, W. Hu, C. Li and Z. Liu, *Anal. Chem.*, 2015, DOI: 10.1021/acs.analchem.5b00172; (d) M. Gao, F. Yu, H. Chen and L. Chen, *Anal. Chem.*, 2015, DOI: 10.1021/ac5044237.
- R. Weissleder, *Nat. Biotechnol.*, 2001, **19**, 316.
- (a) T. Ueno, Y. Urano, H. Kojima and T. Nagano, *J. Am. Chem. Soc.*, 2006, **127**, 10640; (b) F. Yu, P. Li, G. Li, G. Zhao, T. Chu and K. Han, *J. Am. Chem. Soc.*, 2011, **133**, 11030.
- Y. Kimura, Y. Mikami, K. Osumi, M. Tsugane, J. Oka and H. Kimura, *FASEB J.*, 2013, **27**, 2451.
- (a) M. Iciek and L. Włodek, *Pol. J. Pharmacol.*, 2001, **53**, 215; (b) M. Iciek, G. Chwatko, E. Lorenc-Koci, E. Bald and L. Włodek, *Acta Biochim. Pol.*, 2004, **51**, 815; (c) P. J. Włodek, M. B. Iciek, A. Milkowski and O. B. Smolenski, *Clin. Chim.*



- Acta*, 2001, **304**, 9; (d) T. Togawa, M. Ogawa, M. Nawata, Y. Ogasawara, K. Kawanabe and S. Tanabe, *Chem. Pharm. Bull.*, 1992, **40**, 3000; (e) X. Shen, C. Pattillo, S. Pardue, S. Bir, R. Wang and C. Kevil, *Free Radicals Biol. Med.*, 2011, **50**, 1021; (f) Z. Jiang, C. Li, M. L. Manuel, S. Yuan, C. G. Kevil, K. D. McCarter, W. Lu and H. Sun, *PLoS One*, 2015, **10**, e0117982.
- 13 B. Predmore, D. Lefer and G. Gojon, *Antioxid. Redox Signaling*, 2012, **17**, 119.
  - 14 C. Winterbourn, *Nat. Chem. Biol.*, 2008, **4**, 278.
  - 15 N. Francoleon, S. Carrington and J. Fukuto, *Arch. Biochem. Biophys.*, 2011, **516**, 146.
  - 16 (a) J. Toohey, *Anal. Biochem.*, 2011, **413**, 1; (b) Y. Kimura, Y. Mikami, K. Osumi, M. Tsugane, J. Oka and H. Kimura, *FASEB J.*, 2013, **27**, 2451.
  - 17 (a) K. Pu, A. Shuhendler and J. Rao, *Angew. Chem., Int. Ed.*, 2013, **52**, 10325; (b) E. Hecker and R. Schmidt, *Fortschr. Chem. Org. Naturst.*, 1974, **31**, 377.
  - 18 X. Zhu, S. Liu, Y. Liu, S. Wang and X. Ni, *Cell. Mol. Life Sci.*, 2010, **67**, 1119.
  - 19 V. Lin, A. Lippert and C. Chang, *Proc. Natl. Acad. Sci. U. S. A.*, 2013, **110**, 7131.
  - 20 X. Jing, F. Yu and L. Chen, *Chem. Commun.*, 2014, **50**, 14253.